Signature of Self-organized Criticality in Flaring Current Sheets

Yue Zhang (张月)[1], Rui Liu (刘睿)[1*]

[1,*]University of Science and Technology of China; **zhangyue137@mail.ustc.edu.cn**, rliu@ustc.edu.cn

Abstract: In solar flares, magnetic reconnection is key to restructuring the coronal magnetic fields and converting magnetic free energy into other forms of energies. The footpoints of newly reconnected magnetic flux tubes are mapped by chromospheric flare ribbons. The ribbons hence provide clues for structures of, and reconnection processes in, the coronal current sheet, which are still poorly understood. Here we adopt the UV (1600 Å and 1700 Å) filters of AIA/SDO to study the detailed evolution of flare ribbons for a sample of 10 two-ribbon flares. We extract flare ribbons based on the variances of AIA 1600/1700. We find that the frequency distribution for waiting times of the identified pixels on the flare ribbons is well consistent with the theoretical expectation of the SOC model, but the frequency distributions for flaring duration, peak intensity, area under the light curve, and magnetic field strength of the identified pixels generally deviate from power laws and the SOC expectations. These results suggest that time-wise an avalanche process might be ongoing in the flaring current sheet.

Introduction

The aim of SOC: (Bak, Tang and Wiesenfeld, 1987, **BTW** Model)

- Unify the **spatial fractals** and **fractals in time** ubiquitous in the nature.
- Explain the **$1/f$ power spectra**, characterized by a power-law function: $P(\nu) \propto \nu^{-1}$ (pink noise).

The definition of SOC:

- **Original** (BTW Model, 1987)

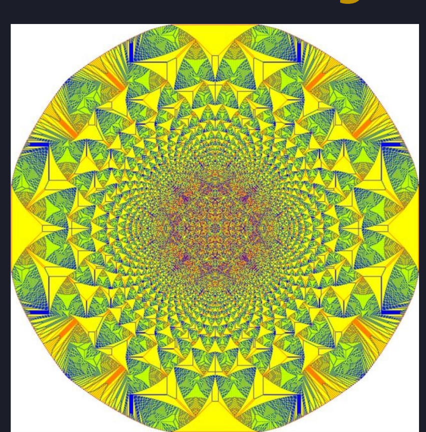

Scale invariance
Self-similarity

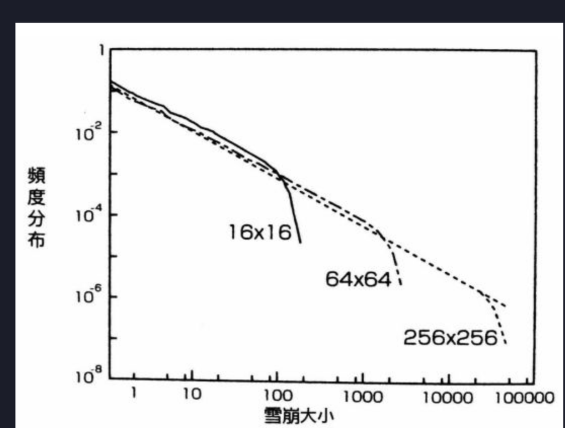

Power-law occurrence frequency distributions

- **Updated** (Pruessner 2012)

Criticality in	SOC	Phase Transitions
Scale invariance at the critical point	• Yes	• Yes
Tuning (adjustment)	• Self-tuning • Rely on its own dynamics to evolve	• Depend on the external adjustment

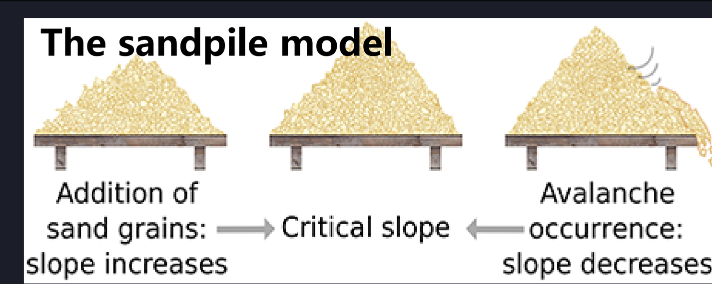

- **More practical and physics-based** (Aschwanden 2014)

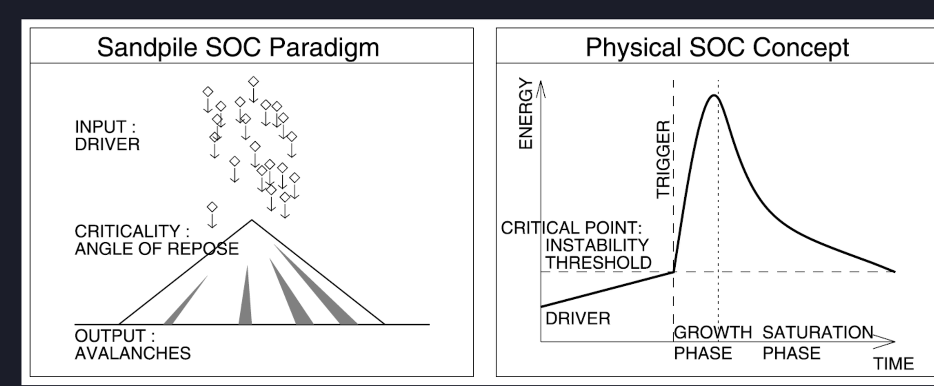

- **Driver:** slowly and continuous
- **Critical point:** a system-wide "instability threshold"
- **Avalanches:** nonlinear energy dissipation events and detectable
  - Occur on whenever and wherever a local instability threshold exceeded.
  - Produce scale-free, fractal-diffusive, and intermittent avalanches with powerlaw-like size distributions of these observables, a hallmark of SOC.

Methods

Flare ribbons identification:

- Extraction of flare ribbons based on variance distribution (AIA 1600/1700 data).
- Variance distribution with two humps: Background and FRs.

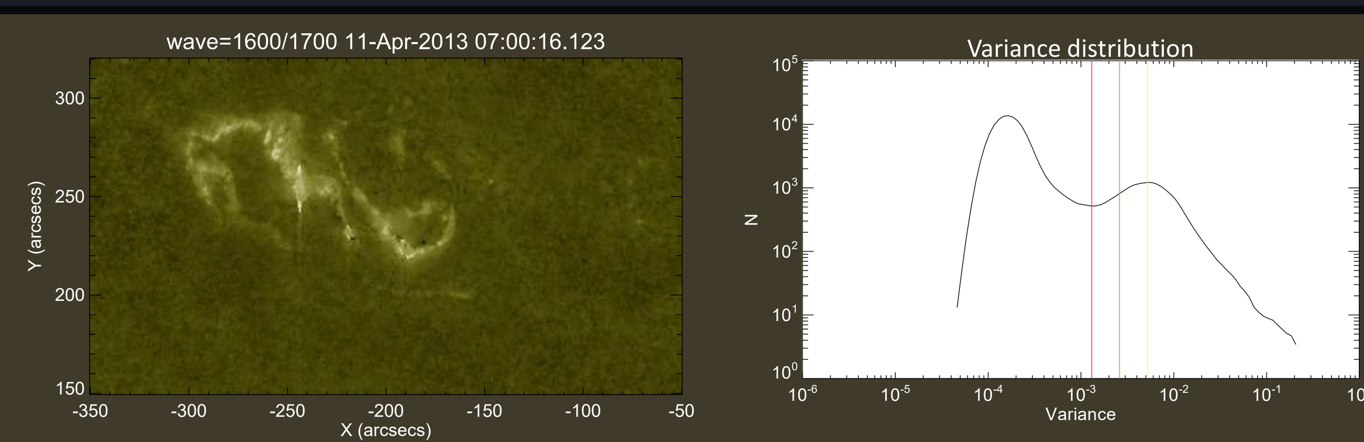

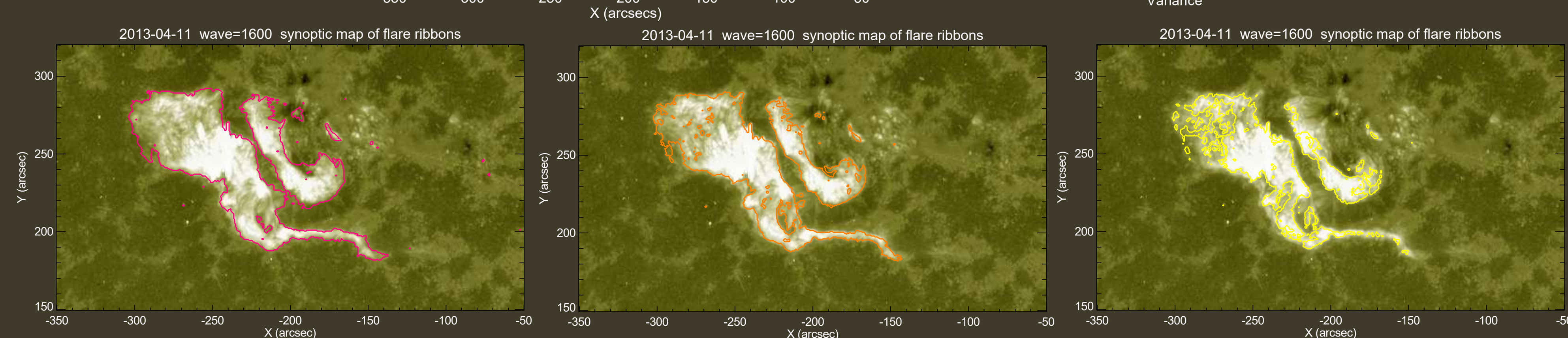

Physical parameters:

- The waiting time: $\boldsymbol{WT}$
- The duration of brightening ($\frac{1}{2}$ peak): $\boldsymbol{T}$
- The peak intensity: $\boldsymbol{P}$
- The area under light curve: LA
- The magnitude of radial magnetic field: $\boldsymbol{B}_R$ (positive $\boldsymbol{B}_{RP}$; negative $\boldsymbol{B}_{RN}$)

The theoretical values: (Aschwanden 2012)

$$d = 2, \beta = 1, \gamma = 1$$

$$D_2 = \frac{D_{2,min} + D_{d,max}}{2} = 1.5$$

- $\alpha_{WT} = \alpha_T = 1 + \frac{(d-1)\beta}{2} = 1.5$
- $\alpha_P = 1 + \frac{(d-1)}{\gamma d} = 1.5$
- $\alpha_{LA} = \alpha_E = 1 + (d-1)/(\gamma D_d + 2/\beta) = 1.29$
- $\alpha_B = 1 + \frac{(d-1)}{\gamma D_d} = 1.67$

- The maximum likelihood estimator (MLE) & The Kolmogorov-Smirnov (KS) test.

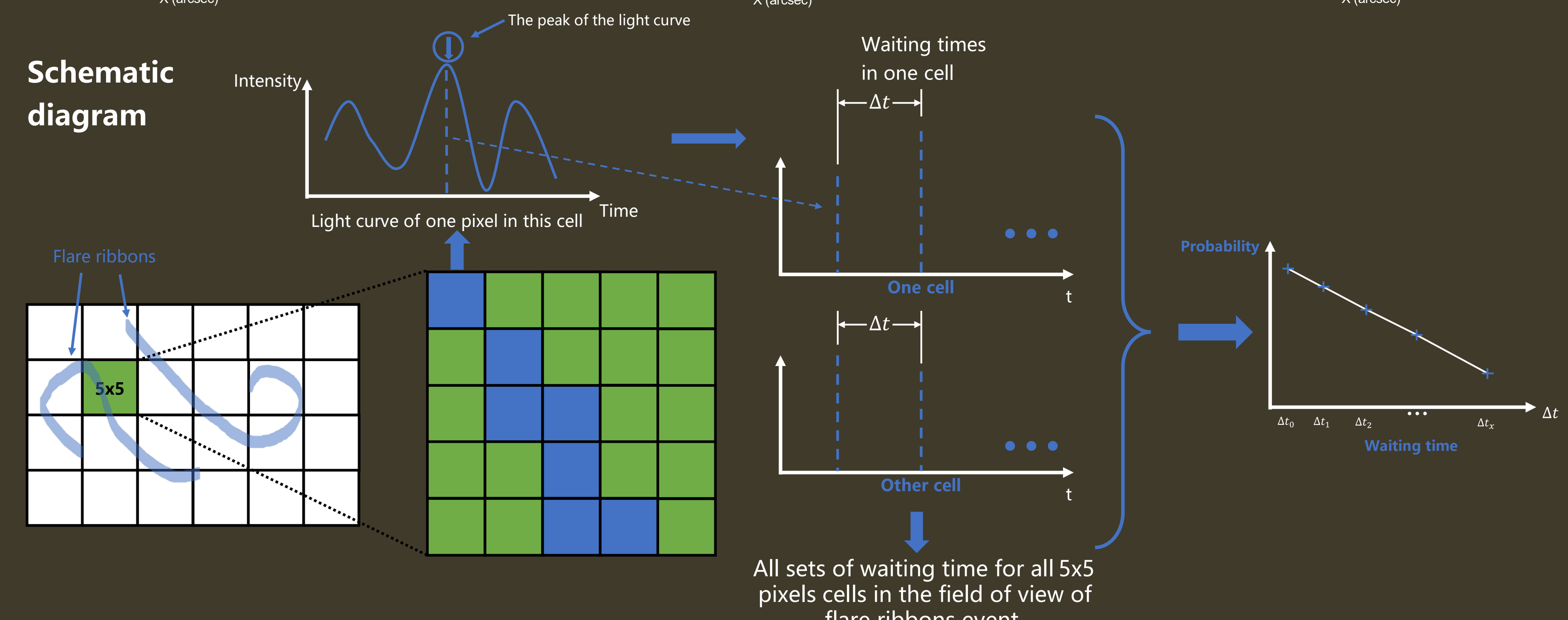

Conclusions

- Identifying flare ribbons by analyzing the variance distribution of the AIA 1600/1700 and studied light curves of each brightening point on the flare ribbons to calculate the size distributions of 5 physical parameters.
- Showing the power-law-like size distributions of WTDs, whose power-law indices are consistent with the theoretical values of the FD-SOC model. These are evidence arguing strongly for the presence of SOC processes (rather than MHD turbulence or non-Poisson process) in the flaring current sheet.
- The power-law index of the WTD of flaring pixels in high spatial resolution IRIS data is also consistent with the SOC model.
- Time-wise an avalanche process might be ongoing in the flaring current sheet, reflected in the evolution of flare ribbons. But in other aspects, e.g., space- and energy-wise, this avalanche is likely modulated by other physical processes.

Results

	Event	α_{WT} (p-value)	α_T (p-value)	α_P (p-value)	α_E (p-value)	α_{BP} (p-value)	α_{BN} (p-value)
1	2011.03.09	$-1.73^{+0.03}_{-0.10}$ (1.00)	$-2.44^{+0.09}_{-0.17}$ (0.99)	$-2.84^{-0.09}_{+0.14}$ (0.00)	$-2.62^{+0.15}_{+0.26}$ (0.00)	$-1.63^{+0.02}_{-0.02}$ (0.00)	$-1.26^{-0.00}_{-0.01}$ (0.00)
2	2013.04.11	$-1.92^{+0.07}_{-0.04}$ (1.00)	$-2.33^{+0.16}_{-0.14}$ (0.89)	$-2.25^{-0.05}_{+0.21}$ (0.00)	$-2.63^{-0.01}_{+0.11}$ (0.00)	$-2.03^{+0.02}_{-0.01}$ (0.01)	$-1.54^{-0.03}_{+0.03}$ (0.00)
3	2014.01.31	$-2.00^{+0.03}_{-0.06}$ (1.00)	$-2.46^{+0.10}_{-0.11}$ (0.84)	$-2.14^{-0.04}_{+0.10}$ (0.00)	$-2.33^{-0.04}_{+0.07}$ (0.00)	$-2.40^{+0.00}_{-0.02}$ (0.01)	$-1.82^{-0.00}_{+0.00}$ (0.00)
4	2014.02.04	$-1.75^{+0.00}_{-0.02}$ (1.00)	$-1.00^{+0.00}_{-0.00}$ (1.00)	$-1.97^{-0.06}_{+0.06}$ (0.00)	$-2.42^{-0.03}_{+0.10}$ (0.01)	$-1.64^{+0.01}_{+0.00}$ (0.00)	$-1.24^{+0.01}_{-0.00}$ (0.00)
5	2014.09.10	$-1.58^{+0.04}_{-0.05}$ (0.93)	$-1.87^{+0.02}_{-0.05}$ (0.58)	$-1.74^{-0.04}_{+0.07}$ (0.00)	$-2.15^{-0.02}_{+0.04}$ (0.00)	$-1.32^{-0.00}_{+0.01}$ (0.00)	$-1.54^{+0.00}_{+0.01}$ (0.00)
6	2015.06.22	$-1.59^{+0.03}_{-0.03}$ (1.00)	$-2.05^{+0.04}_{-0.05}$ (0.63)	$-1.91^{-0.05}_{+0.14}$ (0.00)	$-2.34^{-0.02}_{+0.02}$ (0.00)	$-1.40^{-0.01}_{+0.03}$ (0.00)	$-1.54^{-0.01}_{+0.01}$ (0.00)
7	2015.11.04	$-1.56^{+0.05}_{-0.07}$ (0.88)	$-2.02^{+0.02}_{-0.02}$ (0.31)	$-1.94^{-0.04}_{+0.04}$ (0.00)	$-2.28^{-0.05}_{+0.04}$ (0.00)	$-1.50^{-0.00}_{+0.00}$ (0.00)	$-1.53^{-0.00}_{+0.00}$ (0.00)
8	2016.12.05	$-2.09^{+0.04}_{-0.05}$ (1.00)	$-2.18^{+0.02}_{-0.03}$ (0.81)	$-2.22^{-0.03}_{+0.03}$ (0.00)	$-2.82^{-0.01}_{+0.02}$ (0.00)	$-1.65^{-0.00}_{+0.01}$ (0.00)	$-2.04^{+0.04}_{-0.03}$ (0.16)
9	2021.10.28	$-2.11^{+0.01}_{-0.01}$ (1.00)	$-2.43^{+0.03}_{-0.05}$ (0.99)	$-2.44^{-0.02}_{+0.02}$ (0.00)	$-2.43^{-0.06}_{+0.05}$ (0.00)	$-1.60^{+0.00}_{-0.00}$ (0.00)	$-1.73^{-0.00}_{-0.00}$ (0.00)
10	2023.11.28	$-1.81^{+0.02}_{-0.05}$ (1.00)	$-1.91^{+0.03}_{-0.06}$ (0.39)	$-2.22^{-0.04}_{+0.07}$ (0.00)	$-3.18^{-0.11}_{+0.06}$ (0.00)	$-1.20^{-0.01}_{+0.01}$ (0.00)	$-1.50^{-0.00}_{-0.00}$ (0.00)

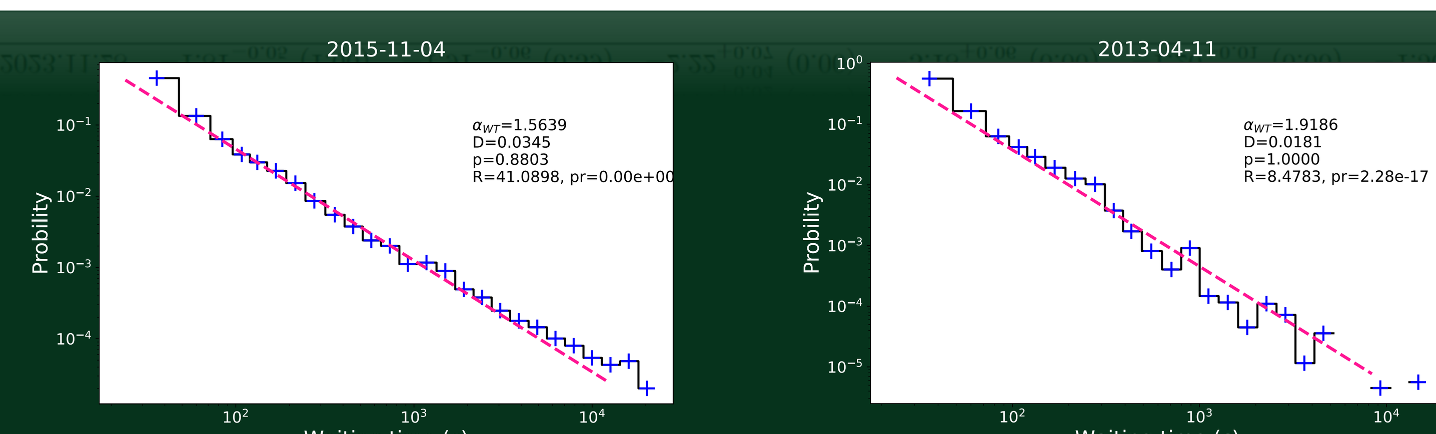

High spatial resolution IRIS data